

Mateusz OTTO*, Aleksandra FIOŁEK**, Sławomir ZIMOWSKI***

INFLUENCE OF A STEEL SUBSTRATE SURFACE ROUGHNESS ON THE MECHANICAL PROPERTIES OF A PEEK COATING DEPOSITED WITH THE ELECTROPHORETIC METHOD

WPLYW CHROPOWATOŚCI POWIERZCHNI PODŁOŻA ZE STALI KONSTRUKCYJNEJ NA WŁAŚCIWOŚCI MECHANICZNE POWŁOKI PEEK OSADZONEJ ELEKTROFORETYCZNIE

Key words:	coating, PEEK, mechanical properties, surface roughness of substrate, electrophoretic deposition method.
Abstract:	The mechanical properties, adhesion and roughness of polymer coatings depend on many factors, including the unevenness of the substrate surface. Nevertheless, the influence of the substrate surface roughness is related to the coating type and substrate material and the used deposition method. Therefore, the effect of the surface roughness of a structural steel substrate on the mechanical properties of a PEEK coating is ambiguous. The indentation tests conducted show that, at a specific load of the indenter, the roughness of the steel substrate surface does not significantly affect the Vicker's hardness of the tested PEEK coatings. The average Vicker's hardness and elastic modulus are approximately 300 MPa and 5.6 Gpa, respectively, at the lowest of the applied loads, regardless of the surface roughness level of the steel substrate. Nevertheless, the surface roughness of the steel substrate after fine grinding of Ra = 0.21 μm, compared to the polished one with Ra = 0.005 μm, meant that adhesion improved, and the scratch hardness increased by approximately 130 to 370 [MPa] of the PEEK coating.
Słowa kluczowe:	powłoka, PEEK, właściwości mechaniczne, chropowatość powierzchni podłoża, metoda elektroforezy.
Streszczenie:	Właściwości mechaniczne, przyczepność oraz chropowatość powłok polimerowych zależą od wielu czynników, a w tym od nierówności powierzchni podłoża. Niemniej jednak wpływ wielkości chropowatości powierzchni podłoża okazuje się być związany z rodzajem materiału powłokowego i podłoża oraz zastosowaną metodą osadzania. Wobec tego oddziaływanie chropowatości powierzchni podłoża ze stali konstrukcyjnej na właściwości mechaniczne powłoki PEEK osadzonej elektroforetycznie nie jest jednoznaczny. Przeprowadzone badania indentacyjne wskazują, że przy określonym obciążeniu wgłębnika chropowatość powierzchni stalowego podłoża nie wpływa znacząco na twardość Vickers'a badanych powłok PEEK. Średnia twardość Vickers'a i modułu sprężystości wynosi odpowiednio ok. 300 MPa i 5.6 GPa przy najmniejszym z zastosowanych obciążeń, niezależnie od mikronierówności powierzchni stalowego podłoża. Nie mniej jednak większa chropowatość powierzchni stalowego podłoża po szlifowaniu dokładnym rzędu Ra = 0.21 μm, względem polerowanego o Ra = 0.005 μm, przełożyła się na polepszanie adhezji i spowodowała wzrost twardości zarysowania powłoki PEEK z ok. 130 do 370 [MPa].

INTRODUCTION

A natural stage in the development of any solution is its optimisation in terms of specific criteria. In industry, one of the most important criteria is

the economic indicator. Hence, in the machinery sector, people are looking for ways to maintain the effectiveness of cooperating elements and, at the same time, reduce operating costs. Currently, the most cost-effective solution that provides the

* ORCID: 0000-0001-5135-4296. AGH University of Science and Technology, Faculty of Metals Engineering and Industrial Computer Science, Mickiewicza 30 Ave., 30-054 Cracow, Poland.

** ORCID: 0000-0001-5977-1481. AGH University of Science and Technology, Faculty of Metals Engineering and Industrial Computer Science, Mickiewicza 30 Ave., 30-054 Cracow, Poland.

*** ORCID: 0000-0002-7348-8751. AGH University of Science and Technology, Faculty of Mechanical Engineering and Robotics, Mickiewicza 30 Ave., 30-059 Cracow, Poland.

desired properties to the kinematic nodes is the application of various types of anti-wear coatings, which, at the same time, improves the sliding properties. Nevertheless, the use of coatings requires careful preparation of the substrate on which the coating is deposited. It is estimated that 30% of the total cost of coating deposition is the process involved in preparing the substrate. This turns out to be particularly important when using coatings for slide bearings due to their application's common and elementary nature in mechanical engineering.

In the group of polymeric materials that are currently widely used in the construction of slide bearings, polyetheretherketone (PEEK) is of great importance [L. 1, 2]. PEEK is a semi-crystalline thermoplastic polymer which, in relation to other polymers, is characterised by excellent mechanical and tribological properties and resistance to increased temperature. Therefore, it is used both as a construction material for monolithic elements and shells of plain bearings. In the case of coatings made of PEEK microparticles, the determining elastic modulus (E_{TP}) is 5.5 GPa, and the Vicker's hardness (H_{TP}) ranges from 100 to 380 MPa, while the scratch hardness (H_{sc}) reaches values up to 300 MPa [L. 3–7]. Moreover, PEEK coatings form an excellent tribological pair due to their low coefficient of sliding friction (f_w), both dry (0.19–0.47) and lubricated (0.12–0.13) in the point contact [L. 3–5, 7–9]. At the same time, they are distinguished by good adhesion to the substrate in terms of the scratch friction coefficient ($f_{sc} = 0.15–0.43$) [L. 7, 10, 11].

Due to the wide range of external forces in the bearing systems, the wear mechanism of the coatings depends on the contact characteristics of the mating surfaces. In the case of loads with non-exerting ranges, the influence of the substrate on the operating conditions in the kinematic node depends exclusively on the type of coating material. However, when the stresses cause interfacial interactions, the substrate deforms and the parameters of the sliding friction change. It is commonly believed that soft coatings are usually insensitive to the geometry of the contact surface due to the capability of significant plastic deformation, which can eliminate significant surface roughness of the substrate [L. 12, 13].

Hence, the results of the pull-off strength test conducted by the team of Paulina Mayer indicate an improvement in the adhesion of polyurethane

coatings with a thickness of 120.1 μm to the substrate made of aluminium alloy (PA11) with an increase in the roughness of the coated surface [L. 14]. It turns out that the adhesion of the coating is nearly four times higher for the surface roughness of the substrate of 2.33 μm than of 0.31 μm (Tab. 1). At the same time, a slight deterioration of adhesion is observed for the surface roughness of the substrate equal to 7.06 μm . Most likely, this is related to the geometry of the substrate surface, which, due to the size of the deviation surface from the mean line, makes it impossible to cover it fully with the coating material [L. 15]. In addition, the reduction in the coating's adhesion may also be a result of the deposition method and substrate material.

Table 1. Pull-off strength (σ) of the polyurethane coating depending on the surface roughness (R_a) of the alumina alloy (PA11) substrate [L. 14]

Tabela 1. Test przyczepności (σ) powłoki poliuretanowej w zależności od chropowatości powierzchni (R_a) podłoża ze stopu aluminium (PA11) [L. 14]

R_a [μm]	0.31	2.33	7.06
σ [MPa]	1.09 \pm 0.08	4.46 \pm 0.21	3.82 \pm 0.35

This is confirmed by the research of the team of Adrian Verforf, which shows differences in the mechanical properties (H , E_r) of the parylene c coating with a thickness of 16.13 μm , depending on the material substrate for different roughness (S_a) of the coated surfaces [L. 16]. The comparison included the hardness (H) and the reduced elastic modulus (E_r), which were determined by the Berkovich indentation test at a load (F_n) of 2 mN (Tab. 2). The obtained results show that the hardness (H) of the parylene c coating on 304 stainless steel and 7620 nickel-plated and 6016 aluminium alloy substrates is similar, despite the differences in the degree of surface roughness (S_a). At the same time, with a similar surface roughness (S_a) of the copper alloy and 304 stainless steel substrates, the hardness (H) of the polymer coating is significantly different. The authors explain that the difference in the mechanical properties of the parylene c coating is due to the substrate surface's machining type and chemical composition, which influenced the polymerisation-deposition process [L. 16]. Moreover, according to several authors, the differences in hardness (H) may be caused by the viscoelastic effects indicated by similar results of the reduced elastic modulus (E_r) [L. 16–18].

Table 2. Hardness (H) and the reduced elastic modulus (E_r) of parlene c coating depending on the surface roughness (S_a) and the substrate material [L. 16]

Tabela 2. Twardość (H) i zredukowany moduł sprężystości (E_r) powłoki parlene c w zależności od chropowatości powierzchni (S_a) oraz materiału podłoża [L. 16]

Material	Aluminium	Cooper	Stainless steel	Nickel steel
S_a [μm]	0.44	0.65	0.39	0.77
H [MPa]	247 \pm 1	272 \pm 1	248 \pm 1	237 \pm 1
E_r [GPa]	4.17 \pm 0.05	4.17 \pm 0.03	3.98 \pm 0.02	3.98 \pm 0.08

Thus, polymer coatings' mechanical properties, adhesion and roughness depend on many factors, including the substrate surface [L. 19]. Nevertheless, the influence of the substrate surface turns out to be related not only to the type of coating material and substrate but also to the applied deposition method [L. 20, 21]. Therefore, the surface roughness effect of a steel substrate on the mechanical properties of a PEEK coating is ambiguous. Hence, in this work, a comparative analysis of mechanical properties was conducted using the instrumental method of pressing the Vicker's indenter and a scratch test with a Rockwell C indenter. The Vicker's hardness (H_{IT}) and the elastic modulus (E_{IT}) were determined during an indentation test, and the adhesion of the coating to the substrate in relation to the scratch friction coefficient (f_s) and the scratch hardness (H_{sc}) were determined based on the scratch test [L. 22].

DEPOSITION OF PEEK COATINGS

In order to make the PEEK coating, Victrex grade-type 708 PEEK- (PEEK-m) microparticles with a grain size of 10 μm were purchased from GmbH (Hofheim am Taunus, Germany). According to the manufacturer's data, the density of the PEEK powder is 1.32 g/cm^3 , the elastic modulus is 4.3 GPa, and the melting and glass transition points are 374°C and 157 °C, respectively [L. 23]. The substrate was made of a C45 steel bar ISO 683-1 1987, purchased from Gomar Steel, which has an elastic modulus (E) equal to 210 GPa and Brinell hardness (H_{ITB}) of 2255 MPa, according to the manufacturer's datasheet. The 35 mm diameter section was processed by turning and was then divided into 15 discs which were 3 mm thick. For the tests, five types of disc differing in surface roughness were prepared, which were obtained by: rough

grinding (C2), fine grinding (C1) and polishing (P) (Fig. 1). The surface topology was investigated with a Filmetrics PROFILM 3D optical profilometer (USA) based on the ISO 4287 and ISO 25178 standards. The scanning included 12 measurements of a 2x2 [mm] lens with 50x magnification (Nikon CF IC Epi Plan) in randomly selected areas on the disc surface. Surface roughness is characterised by parameters describing the arithmetic mean deviation of the profile from the mean line (R_a) and the deviation of the roughness height from the reference plane (S_a), i.e. the parameters commonly used in the description of the surface.

The deposition process was carried out using the electrophoresis (EPD) method. For this purpose, 1.5 g of PEEK 708 microparticles were mixed while calculating it for every 50 ml of 99.8% pure ethyl alcohol. In order to reduce the probability of possible particle thickening in the mixture, ultra-sonic bathing was performed with a Polsonic Sonic-3 (Poland) washer for 20 minutes. Moreover, immediately before starting the deposition process, the colloidal suspension was homogenised with an IKA C-MAG HS 4 digital magnetic mixer (Germany) with a rotational speed of 300 rpm for 10 min. The C2, C1 and P substrates (anode) were placed successively in the mixture prepared in this way at a distance of 10 mm from the fully immersed fragment of austenitic stainless steel ISO A2 of dimensions 97x15x1 [mm], which serves as a counter electrode (cathode). In the created two-electrode system, a voltage of 70 V was applied using a multimode EX752M PSU (Great Britain) power supply, for which the deposition time was 10 s. During the entire process, the colloidal suspension was magnetically stirred at a rotation speed of 20 rpm in order to avoid particle sedimentation. Then, the samples were heated in a Czylok FCF 5SP muffle furnace (Poland) with a temperature increase of 4.5°C/min until reaching 380°C, and this thermal state was maintained for 20 minutes. After this time, the samples were cooled in a furnace at the rate of 2°C/min until room temperature was reached (approx. 21°C). According to the Hamaker equation, the deposited coatings should reach a thickness of 40 μm (eq. 1). In order to verify the above calculations, the thickness of the polymer coating was measured by the contact method using an Anton Paar Step 500 tester with an MCT³ measuring head (Switzerland). Three measurements were taken for each sample along the line originating on the uncoated substrate surface. The measured average thickness of PEEK

$$m = \int_0^t \mu \cdot E \cdot C \cdot A \cdot dt \quad (1)$$

m : deposited mass

μ : electrophoretic mobility of particles

E : applied electric field

C : particle concentration in suspension

A : electrode area

t : deposition time

coatings deviates slightly from the calculated value (1) and is approximately 36, 43, and 39 [μm] for the C2, C1 and P substrates, respectively. The surface topology of the produced PEEK coatings was measured similarly to the substrates (**Fig. 2**).

machining type	rough grinding (C2)	fine grinding (C1)	polishing (P)
surface roughness	Ra = 0.436 ± 0.049 Sa = 1.103 ± 0.164	Ra = 0.211 ± 0.034 Sa = 0.744 ± 0.041	Ra = 0.005 Sa = 0.055 ± 0.011

machined surface



Fig. 1. Shape and surface roughness of the steel substrate depending on machining type

Rys. 1. Kształt oraz chropowatość powierzchni stalowego podłoża w zależności od rodzaju obróbki

coating symbol	PEEK (C2)	PEEK (C1)	PEEK (P)
surface roughness	Ra = 0.075 ± 0.013 Sa = 1.474 ± 0.172	Ra = 0.066 ± 0.008 Sa = 1.127 ± 0.113	Ra = 0.054 ± 0.014 Sa = 1.028 ± 0.201

grip zone

deposited PEEK coating

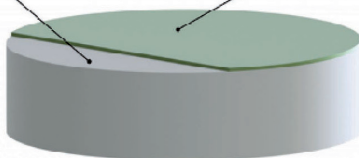


Fig. 2. Surface roughness of the PEEK coating depending on the type of substrate machining

Rys. 2. Chropowatość powierzchni powłoki PEEK w zależności od rodzaju obróbki podłoża

EXECUTION OF INDENTATION AND SCRATCH TESTS

An instrumental method of pressing the Vicker's indenter was performed using the Micro-Combi

Tester (MCT) of CSM Instruments (Switzerland), and a scratch test with a Rockwell C indenter was performed using an Anton Paar Step 500 with an MCT³ measuring head (Switzerland). All tests were carried out at room temperature (approx. 21°C) and 50% relative humidity.

Indentation test

The Vicker's indentation tests were carried out in accordance with the ISO 14577-4: 2016 standard [L. 24]. The Vicker's indenter was pressed with a linearly increasing load (F_n) of 50, 100 and 200 [mN], with the maximum value reached after 30 s (**Fig. 3**). The maximum load (F_n) was maintained for 15 s. The obtained dependence of the indenter

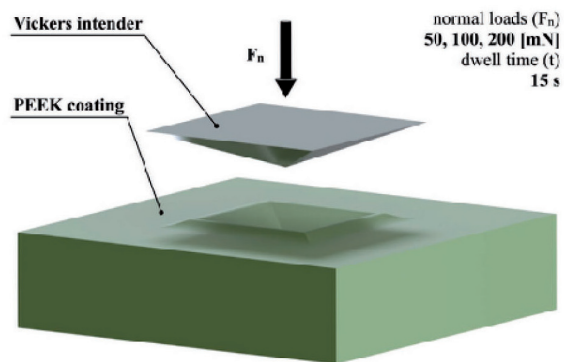


Fig. 3. Vickers hardness test

Rys. 3. Test twardości Vickers'a

penetration on the value of the normal force (F_n) enabled analysis to be performed of the load and unload curves in the indentation test. On their basis, the gradient of the tangent to the retract curve (a) and the maximum penetration depth (d_{max}) were determined for each load (F_n) used in the test. By using the defined parameters and developed mathematical models, the dependencies describing the indentation elastic modulus (E_{IT}) and Vicker's hardness (H_{IT}) were derived, enabling the individually positioned tangent to be adjusted to the retract curve (a) for a single measurement and thus a smaller dispersion of test results (eq. 2–6) [L. 25–30]. Therefore, the determined mechanical properties (H_{IT} , E_{IT}) are the arithmetic mean of a series of 12 measurements for each of the assumed loads (F_n).

$$E = (1 - \nu^2) \cdot \left[\frac{1}{E_r} - \frac{1 - (\nu_i)^2}{E_i} \right]^{-1} \quad (2)$$

$$E_r = \frac{2}{\pi} \cdot \frac{a}{\sqrt{A_p}} \quad (3)$$

$$d_c = d_{max} - \epsilon \cdot \frac{F_{nmax}}{a} \quad (4)$$

$$A_p = 4 \cdot (d_c)^2 \cdot \left[\tan\left(\frac{\alpha}{2}\right) \right]^2 \quad (5)$$

$$E_{IT} = (1 - \nu^2) \cdot \left[\frac{4}{\sqrt{\pi}} \cdot \frac{1}{a} \cdot \left(d_{max} - \epsilon \cdot \frac{F_{nmax}}{a} \right) \cdot \tan\left(\frac{\alpha}{2}\right) - \frac{1 - (\nu_i)^2}{E_i} \right]^{-1} \quad (\text{from 2, 3, 4, 5})$$

$$H_{IT} = \frac{F_{nmax}}{A_p} \quad (6)$$

$$H_{IT} = \frac{1}{4} \cdot \frac{F_{nmax}}{\left(d_{max} - \epsilon \cdot \frac{F_{nmax}}{a} \right)^2 \cdot \left[\tan\left(\frac{\alpha}{2}\right) \right]^2} \quad (\text{from 5, 6})$$

F_{nmax} : maximum normal force

d_{max} : maximum indentation depth

d_c : contact indentation depth

A_p : projected contact area

a : gradient of the tangent to retract curve

ϵ : constant of indenter geometry (for Vickers tip = 0.75)

α : angle of the indenter tip (for Vickers tip = 136°)

ν : Poisson's ratio of the specimen (for PEEK = 0.413 – 0.427)

ν_i : Poisson's ratio of the Vickers tip (0.07)

E : elastic modulus of the specimen

E_i : elastic modulus of the indenter tip (for Vickers tip = 1140 GPa)

E_r : reduced elastic modulus

Scratch test

Scratch tests were performed with a Rockwell C indenter based on the ASTM D7027-13 standard [L. 31]. The tests were carried out with a load (L_n) which increased linearly the range from 0 to 30 N and from 0 to 20 N, along the scratch length of 5 mm with a relative indenter feed rate of 5 mm/min (Fig. 4). Basing on the measurements of the scratch geometry using the Filmetrics PROFILM

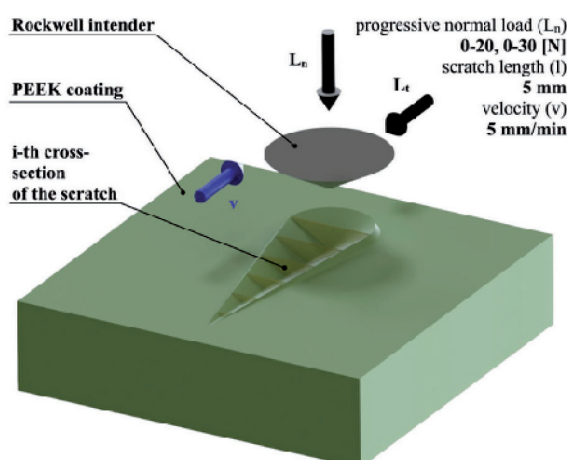


Fig. 4. Scratch test

Rys. 4. Test zarysowania

3D optical profilometer (USA), a three-dimensional scratch model was built. Using the Gwyddion software, the created scratch model was analyzed within the section of the scratch trough limited by the occurrence of the load that causes cohesive failure of the coating (L_{c1}). The analysis included 8 scratch cross-sections for which, proportionally to the total scratch length, the achieved normal force (L_n), the maximum width (w_{max}) of the trough and the shape of the formed crater were determined. On this basis and in relation to the test parameters, mathematical relationships describing the scratch hardness (H_{sc}) and the scratch friction coefficient (f_{sc}) measured along the entire length of the scratch determined were developed (eq. 7–8).

$$H_{sc} = \frac{2}{3 \cdot \pi} \cdot \sum_{i=1}^6 \frac{L_n^i}{(w_{max}^i)^2} \quad (7)$$

$$f_{sc} = \frac{L_t}{L_n} \quad (8)$$

L_n^i : normal load achieved in i -th cross-section area of the scratch

L_n : normal load measured in every 0.063 sec. of test

L_t : tangential load measured in every 0.063 sec. of test

w^i : width of the trough observed in i -th cross-section area of the scratch

RESULTS OF MECHANICAL TESTS AND SCRATCH RESISTANCE OF THE PEEK COATING

The performed indentation test does not show any significant influence of the surface roughness parameters (R_a , S_a) on the PEEK coating's mechanical properties (H_{IT} , E_{IT}). The maximum penetration depths (d_{max}) for the PEEK/C2, PEEK/C1, and PEEK/P coatings at the load (F_n) equal to 200 mN were respectively 5.8, 5.9 and 5.6 [μm], while with 100 and 50 [mN] were 4, 3.9 and 3.7 as well as 2.8, 2.7 and 2.6 [μm] respectively.

In the case of the scratch test, the influence of the surface roughness on the test results can be observed. The maximum scratch depth (d_{max}) for each of the samples is equal to the thickness of the PEEK/C2, PEEK/C1 and PEEK/P coatings, regardless of the linearly increasing normal force (L_n) which was used in the tests.

Vicker's hardness and elastic modulus

The determined Vicker's hardness values (H_{IT}) of the tested PEEK coatings are similar to each other, regardless of the substrate type (Fig. 5). On the other hand, a small difference in the average values (H_{IT}) is also the result of a small difference in the thickness of the PEEK/C2, PEEK/C1 and PEEK/P coatings, which influenced the deformation ability of the coating-substrate system. At the same time, the impact of the substrate material on the Vicker's hardness (H_{IT}) of the tested PEEK coatings cannot be eliminated due to the maximum penetration depth (d_{max}) of the indenter in the performed tests.

This is confirmed by the results of the elastic modulus (E_{IT}) (Fig. 6). The performed tests show a noticeably higher value (E_{IT}) for the PEEK/C2 coating compared to the PEEK/C1 and PEEK/P coatings at the load (F_n) of 200 mN. This difference is visible not only when comparing it to the background of the similar elastic modulus of PEEK/C1 and PEEK/P coatings at a load (F_n) equal to 200 mN, but also in relation to other results (E_{IT}), which are comparable to loads (F_n) of 50 and 100 [mN] regardless of the substrate type. At the same time, an increase in the elastic modulus (E_{IT}) is observed with the increased applied load (F_n) in the indentation test of PEEK coatings. Despite a slight increase in the value (E_{IT}) at a load (F_n) of 100 mN versus 50 mN, no significantly higher Vicker's hardness (H_{IT}) was found for the PEEK/C2, PEEK/C1 and PEEK/P coatings. On this basis, it can be

assumed that the roughness of the substrate does not affect the results of the indentation tests if the appropriate proportion of the penetration depth to the coating thickness is maintained.

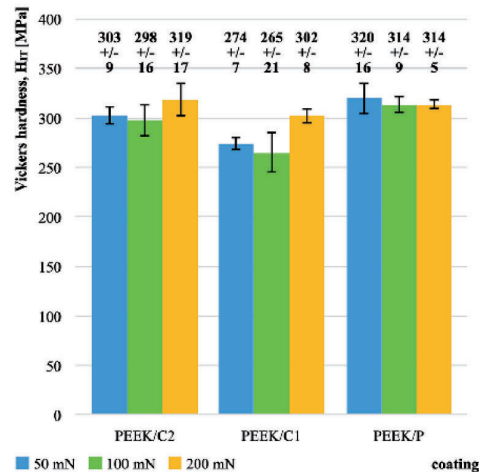


Fig. 5. Results of the Vicker's hardness (H_{IT}) of the PEEK coating depends on degree of the substrate surface roughness

Rys. 5. Wyniki twardości Vickers'a (H_{IT}) powłoki PEEK w zależności od chropowatości powierzchni podłoża

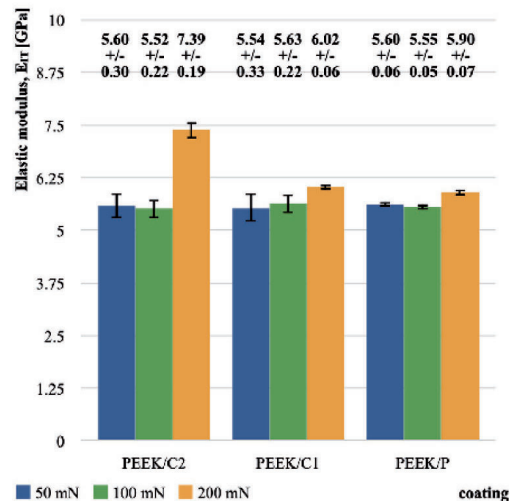


Fig. 6. Results of the elastic modulus (E_{IT}) of the PEEK coating depends on degree of the substrate surface roughness

Rys. 6. Wyniki modułu sprężystości (E_{IT}) powłoki PEEK w zależności od chropowatości powierzchni podłoża

Scratch hardness, coefficient of scratch friction and coating adhesion

The computed scratch hardness (H_{sc}) of the deposited PEEK coatings differs depending on the substrate surface roughness (Fig. 7). At the same time, for each of the samples, the results are comparable for

the indenter load (L_n) from 0 to 30 N and from 0 to 20 N for each of the samples. Nevertheless, in the case of the PEEK/C2 and PEEK/C1 coatings, the values are clearly higher but also more spread in relation to the PEEK/P coating, regardless of the adopted progressive load (L_n). Higher scratch hardness (H_{sc}) proves the lower plastic deformation of PEEK/C2 and PEEK/C1 coatings, and thus the possibility of transferring higher loads.

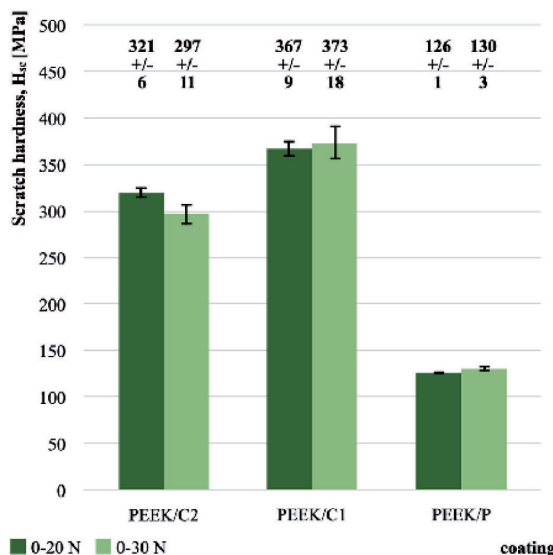


Fig. 7. Results of the scratch hardness (H_{sc}) of the PEEK coating depends on the degree of substrate surface roughness

Rys. 7. Wyniki twardości zarysowania (H_{sc}) powłoki PEEK w zależności od chropowatości powierzchni podłoża

The coefficient of scratch friction (f_{sc}) along the entire scratch path (l) and critical loads (L_{c1} , L_{c2} , L_{c3}) causing the characteristic deterioration of the PEEK coating also indicate a significant influence of the substrate surface roughness on the measured values (Fig. 8, 9). As long as the progressive load (L_n) increases, the Rockwell indenter presents growing resistance, which is the least stable for the PEEK/C1 coating against the PEEK/C2 and PEEK/P coatings. Nevertheless, the change in the scratch friction coefficient (f_{sc}) value corresponds to the appearance of cohesive failure (L_{c1}). That destruction is the result of tensile stress concentration and the plastic deformation of PEEK coatings and appears with similar loads (L_{c1}) in all samples, regardless of the substrate surface roughness (Fig. 10, 11). Further development of the load (L_n) causes a more intensive increase in the scratch friction coefficient (f_{sc}) of the PEEK/P coating compared to the PEEK/C2 and PEEK/

C1 coatings. The resulting cracks affected the substrate, and due to the shear stress generated by the Rockwell indenter, the PEEK coating was locally disbanded inside the trough. The complete discontinuity of all the tested PEEK coatings is observed, while the load required for adhesive failure (L_{c2}) of the PEEK/C2 and PEEK/C1 coatings is significantly higher for the PEEK/P coating (L_{c3}). In addition, extensive losses in the upper parts of the PEEK/P coating are not present in the PEEK/C2 and PEEK/C1 coatings. The size of the defects indicates delamination of the PEEK/P coating (L_{c3}). It is important that this failure occurred directly after cohesive cracks (L_{c1}) and was not preceded by local disbanding of the PEEK coating from the substrate, typical for adhesive failure (L_{c2}).

SUMMARY AND DISCUSSION

The results of Vicker's indentation tests (H_{IT} , E_{IT}) indicate greater repeatability of measurements for PEEK coatings on a steel substrate with a polished (P) surface than for rough and finely-ground (C2, C1) ones. Nevertheless, the machining type did not affect the average Vicker's hardness

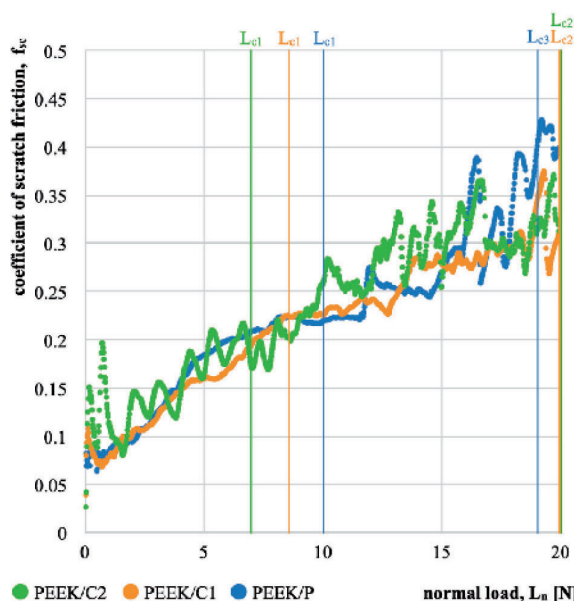


Fig. 8. Coefficient of scratch friction (f_{sc}) and critical loads (L_{c1} , L_{c2} , L_{c3}) determined in the scratch test ($L_n = 0-20$ N) of the PEEK coating depends on the degree of substrate surface roughness

Rys. 8. Wyniki współczynnika tarcia zarysowania (f_{sc}) oraz obciążenia krytyczne (L_{c1} , L_{c2} , L_{c3}) wyznaczone w teście zarysowania ($L_n = 0-20$ N) powłoki PEEK w zależności od chropowatości powierzchni podłoża

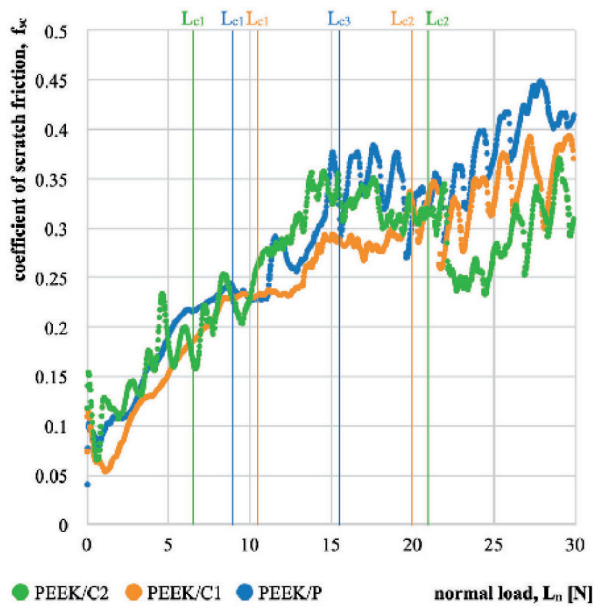


Fig. 9. Coefficient of scratch friction (f_{sc}) and critical loads (L_{c1} , L_{c2} , L_{c3}) determined in the scratch test ($L_n = 0-30$ N) of the PEEK coating depends on the degree of

Rys. 9. Wyniki współczynnika tarcia zarysowania (f_{sc}) oraz obciążenia krytyczne (L_{c1} , L_{c2} , L_{c3}) wyznaczone w teście zarysowania ($L_n = 0-30$ N) powłoki PEEK w zależności od chropowatości powierzchni podłoża

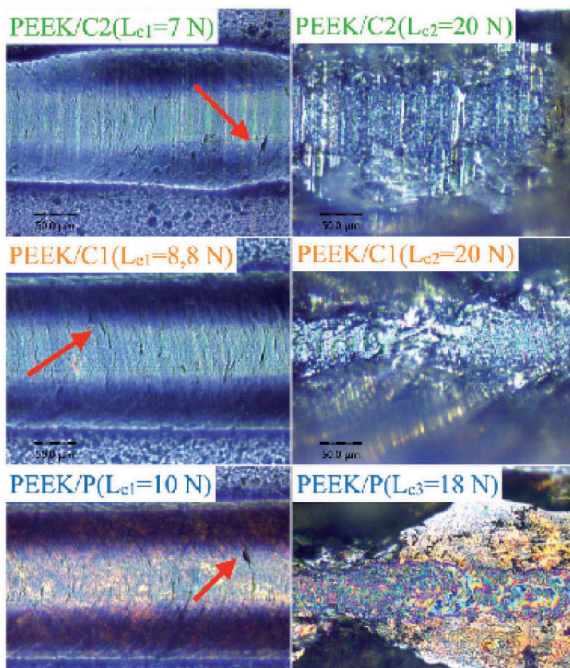


Fig. 10. Track in the scratch test ($L_n = 0-20$ N) at critical loads (L_{c1} , L_{c2} , L_{c3}) of the PEEK coating depends on the degree of substrate surface roughness

Rys. 10. Tor w teście zarysowania ($L_n = 0-20$ N) pod obciążeniami krytycznymi (L_{c1} , L_{c2} , L_{c3}) powłoki PEEK w zależności od chropowatości powierzchni podłoża

(H_{IT}) of the PEEK coatings, which is from 265 to 320 MPa (Tab. 3). The obtained results (H_{IT}) are comparable with the majority of research studies by several authors, however, according to them the values are in a wide range from 100 to 350 MPa [L. 3, 5, 7, 32, 33].

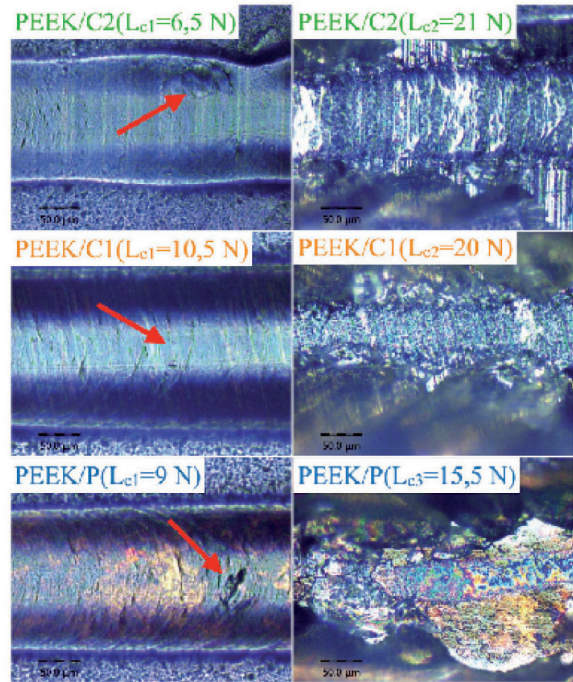


Fig. 11. Track in the scratch test ($L_n = 0-30$ N) at critical loads (L_{c1} , L_{c2} , L_{c3}) of the PEEK coating depends on the degree of substrate surface roughness

Rys. 11. Tor w teście zarysowania ($L_n = 0-30$ N) pod obciążeniami krytycznymi (L_{c1} , L_{c2} , L_{c3}) powłoki PEEK w zależności od chropowatości powierzchni podłoża

Table 3. Vickers hardness (H_{IT}) determined in the indentation test of PEEK coatings depends on the degree of substrate surface roughness

Tabela 3. Twardość Vickers'a (H_{IT}) wyznaczona w teście indentacji powłoki PEEK w zależności od chropowatości powierzchni podłoża

Coating symbol	PEEK/C2	PEEK/C1	PEEK/P	Load (F_n) [mN]
Vickers hardness (H_{IT}) [MPa]	303 ±9	274 ±7	320 ±16	50
	298 ±16	265 ±21	314 ±9	100
	319 ±17	302 ±8	314 ±5	200

The reason for the differences in these values (H_{IT}) for PEEK coatings is the influence of the degree of polymer crystallinity, which is shaped by the applied deposition method and the adopted annealing and cooling process, as well as the

stiffness of the coating-substrate system, which is strongly dependent on the coating thickness [L. 34–38]. In addition, the developed calculation model used in this work enabled the precise determination of the tangent to the unload curve at the moment of elastic recovery in the indentation test conducted individually for every measurement. As a result, it is possible to perform a detailed analysis of the measurement data in the indentation tests of Vicker's hardness (H_{IT}) and elastic modulus (E_{IT}), which reduces the standard deviation of the test results.

Regardless of how the results are determined, the maximum penetration depth (d_{max}) should

not exceed 10% of the coating thickness for a correctly performed measurement. According to the indentation test carried out at the load (F_n) equal to 200 mN, the maximum penetration depth (d_{max}) reached approximately 16.1, 13.7 and 14.4 [%] of the thickness of the PEEK coating deposited on the C2, C1 and P substrates, respectively (Tab. 4). However, for loads (F_n) of 50 and 100 [mN], the quotient of the maximum penetration depth (d_{max}) and the thickness of the PEEK coating are 7.8, 6.3, and 6.7 [%] as well as 11.1, 9.1, and 9.5 [%], respectively, for subsequent C2, C1 and P substrates.

Table 4. Indentation depth (d_{max}) and elastic modulus (E_{IT}) determined in the indentation test of PEEK coatings depends on the degree of substrate surface rough

Tabela 4. Głębokość penetracji (d_{max}) oraz moduł sprężystości (E_{IT}) wyznaczone w teście indentacji powłoki PEEK w zależności od chropowatości powierzchni podłoża

Coating symbol	PEEK/C2		PEEK/C1		PEEK/P		Load (F_n) [mN]
Indentation depth (d_{max}) [μ m]	2.8	(7.8%)	2.7	(6.3%)	2.6	(6.7%)	50
	4.0	(11.1%)	3.9	(9.1%)	3.7	(9.5%)	100
	5.8	(16.1%)	5.9	(13.7%)	5.6	(14.4%)	200
Thickness [μ m]	36		43		39		
Elastic modulus (E_{IT}) [GPa]	5.60 \pm 0.30		5.54 \pm 0.33		5.60 \pm 0.06		50
	5.52 \pm 0.22		5.63 \pm 0.22		5.55 \pm 0.05		100
	7.39 \pm 0.19		6.02 \pm 0.06		5.90 \pm 0.07		200

The thickness of the PEEK coatings causes the discrepancy in the obtained proportions because the maximum penetration depths (d_{max}) are comparable to each other. Despite the failure to fulfil the condition of limiting the maximum penetration depth (d_{max}) in some measurements, no significant influence of substrate material properties on the Vicker's hardness (H_{IT}) of the PEEK coatings was observed. This effect is more evident in the elastic modulus (E_{IT}) results.

This is proved by similar values (E_{IT}) of the PEEK coatings determined at loads (F_n) of 50 and 100 [mN], which are from 5.54 to 5.63 [GPa]. The exception is the elastic modulus (E_{IT}) for the PEEK/C2 coating at a load (F_n) of 200 mN equal to 7.39 GPa, which is noticeably higher than the other results (E_{IT}) with identical measurement parameters. Nevertheless, for this load ($F_n = 200$ mN), an increase in the elastic modulus (E_{IT}) for each sample is observed, indicating the influence of the

substrate material properties. However, for lower maximum penetration depth (d_{max}) with a load (F_n) of 50 and 100 [mN], there is no influence on the substrate material properties, and the values (E_{IT}) are similar to the results of other indentation research studies, according to which the elastic modulus (E_{IT}) of the PEEK coating is 5.4 GPa [L. 7].

Thus, the surface roughness of the steel substrate does not affect the mechanical properties (H_{IT} , E_{IT}) of the PEEK coating, which were determined based on the Vickers indentation test at a specific load. It is concluded that the measured Vicker's hardness (H_{IT}) and elastic modulus (E_{IT}) increase during indentation measurements when the penetration depth (d_{max}) significantly exceeds 10% of the PEEK coating thickness, which is most obvious in the thinnest one (PEEK/C2). This is due to the impact of the surface roughness peaks of the steel substrate during the indentation test.

PEEK coatings have great resistance to scratches, described as scratch hardness (H_{sc}) and the coefficient of scratch friction (f_{sc}). Nevertheless, the results from scratch tests show that both parameters (H_{sc} , f_{sc}) strongly depend on the substrate surface roughness. In the scratch tests with a progressive load from 0 to 20 N and 0 to 30 N, respectively, the average scratch hardness (H_{sc}) of the PEEK/C2 and PEEK/C1 coating is from 297 to 372 MPa and significantly higher in comparison to the PEEK/P value (H_{sc}) from 126 to 130 MPa (**Tab. 5**). The validation of the archived values is confirmed by the research of other authors, according to whom the scratch hardness (H_{sc}) of the PEEK coating is equal to both 113 MPa and 300 MPa, depending on the degree of polymer crystallinity or type of substrate material [**L. 6, 7**]. Therefore, the differences in the obtained results are a consequence of microunevenness in the profile deviation of the substrate surface, with its fluctuation creating a physical barrier to the moving Rockwell C indenter in the scratch test.

Table 5. Scratch hardness (H_{sc}) determined in the scratch test of PEEK coatings depends on the degree of substrate surface roughness

Tabla 5. Twardość zarysowana (H_{sc}) wyznaczona w teście zarysowania powłoki PEEK w zależności od chropowatości powierzchni podłoża

Coating symbol	PEEK/C2	PEEK/C1	PEEK/P	Progressive load (F_n) [mN]
Scratch hardness (H_{sc}) [MPa]	321 ±6	367 ±9	126 ±1	0–20
	297 ±11	373 ±18	130 ±3	0–30

Hence, the scratch friction coefficient (f_{sc}) of the PEEK/C2, PEEK/P, PEEK/C1 coatings changes the course characteristic after the appearance of cohesive failure at the load (L_{c1}) of 6.5, 9 and 10.5 [N], respectively. Further build-up of the load to the appearance of adhesive failure (L_{c2} , L_{c3}) causes a more intense increase in the scratch friction coefficient (f_{sc}) of the PEEK/P coating in relation to the PEEK/C2 and PEEK/C1 coatings,

which is a result of the degree of substrate surface roughness. At the same time, the critical load (L_{c3}) that causes disbanding of the PEEK/P coating is the lowest and equals 15.5 N, while for the PEEK/C2 and PEEK/C1 coatings, it equals 20 and 21 [N], respectively.

The defect size and form of damage indicate the better adhesion of the PEEK coating to the steel substrate after grinding (C2, C1) than polishing (P). The irregularity and the microunevenness of the surface caused enlargement of the basal area contact of the coating with the C2 and C1 substrates, which improved adhesion of the deposited PEEK coatings [**L. 14**].

CONCLUSIONS

The conducted research and its analysis allow the following statements to be formulated:

- the surface roughness of the steel substrate does not affect the Vicker's hardness (H_{IT}) and the elastic modulus (E_{IT}) of the PEEK coating if indenter penetration in the indentation test does not exceed 10% of its thickness,
- the surface roughness of the steel substrate determines the scratch resistance (H_{sc} , f_{sc}) of the PEEK coating,
- the microunevenness increase of the steel substrate surface improves adhesion and increases the scratch hardness (H_{sc}) of the PEEK coating,
- fine grinding (C1) of the surface roughness, $R_a = 0.21$ and $S_a = 0.75$ [μm], is sufficient machining of the steel substrate for PEEK coating deposition with the electrophoresis method.

Acknowledgements

This work was supported by the Polish Ministry of Science and Higher Education under subvention funds for the Department of Machine Design and Exploitation of AGH-UST (AGH grant number 16.16.130.942).

REFERENCES

1. Yeo S.M., Polycarpou A.A.: Tribological performance of PTFE- and PEEK-based coatings under oil-less compressor conditions. *Wear* 2012, 296(1-2), pp. 638-647
2. Lin L., Ecke N., Huang M., Pei X.-Q., Schlarb A. K.: Impact of nanosilica on the friction and wear of a PEEK/CF composite coating manufactured by fused deposition modeling (FDM). *Composites Part B: Engineering* 2019, p. 177.
3. Li J., Liao H., Coddet C.: Friction and wear behavior of flame-sprayed PEEK coatings. *Wear* 2002, 252(9-10), pp. 824-831
4. Zhang G., Li W., Cherigui M., Zhang C., Liao H., Bordes J.-M., Coddet C.: Structures and tribological performances of PEEK (poly-ether-ether-ketone) based coatings designed for tribological application. *Progress in Organic Coatings* 2007, 60(1), pp. 39-44.
5. Zhang C., Zhang G., Ji V., Liao H., Costil S., Coddet C.: Microstructure and mechanical properties of flame-sprayed PEEK coating remelted by laser process. *Progress in Organic Coatings*. *Progress in Organic Coatings* 2009, 66(3), pp. 248-253.
6. Tharajak J., Palathai T., Sombatsompop N.: Scratch Resistance and Adhesion Properties of PEEK Coating Filled with h-BN Nanoparticles. *Advanced Materials Research* 2013, 747, pp. 303-306.
7. Otto M., Zimowski S., Sikora W., Moskalewicz T.: Mechanical and Tribological Analysis of Monolith and Coating Polyetheretherketone. *Tribologia* 2019, 286(4), pp. 73-86.
8. Song J., Liao Z., Wang S., Liu Y., Liu W., Tyagi R.: Study on the Tribological Behaviors of Different PEEK Composite Coatings for Use as Artificial Cervical Disk Materials. *Journal of Materials Engineering and Performance* 2015, 25(1), pp. 116-129.
9. Moskalewicz T., Zimowski S., Fiołek A., Łukaszczyk A., Dubiel B., Cieniek Ł.: The Effect of the Polymer Structure in Composite Alumina/Polyetheretherketone Coatings on Corrosion Resistance, Micro-mechanical and Tribological Properties of the Ti-6Al-4V Alloy. *Journal of Materials Engineering and Performance* 2019, 29(3), pp. 1426-1438.
10. Friedrich K., Sue H. J., Liu P., Almajid A.: Scratch resistance of high performance polymers. *Tribology International* 2011, 44(9), pp. 1032-1046.
11. Lina L., Peib X.-Q., Bennewitz R., Schlarb A. K.: Friction and wear of PEEK in continuous sliding and unidirectional scratch tests. *Tribology International* 2018, 122, pp. 108-113.
12. Hayward I.P., Singer I.L., Seitzman L.E.: Effect of roughness on the friction of diamond on cvd diamond coatings. *Wear* 1992, 157(2), pp. 215-227.
13. Bhushan B., Subramaniam V. V., Malshe A., Gupta B. K., Ruan J.: Tribological properties of polished diamond films. *Journal of Applied Physics*. 74(6), 1993, pp. 4174-4180.
14. Mayer P., Dmitruk A., Jósiewicz M., Gluch M.: Pull-off strength of fiber-reinforced composite polymer coatings on aluminum substrate. *The Journal of Adhesion* 2020, pp. 1-17.
15. Finch C.A.: Adhesion and adhesives technology – an introduction, 2nd ed. AV Pocius. Carl Hanser Gardener Verlag, Munchen, 2002. *Polymer International* 2004, 53(9), pp. 1394-1394.
16. Verwolf A., White G., Poling C.: Effects of substrate composition and roughness on mechanical properties and conformality of parylene C coatings. *Journal of Applied Polymer Science* 2013, 127(4), pp. 2969-2976.
17. Fortin J.B., Lu T.-M.: *Chemical Vapor Deposition Polymerization* 2004.
18. Surmeneva M.A., Vladescu A., Cotrut C.M., Tyurin A.I., Pirozhkova T.S., Shuvarin I.A., Elkin B., Oehr C., Surmenev R.A.: Effect of parylene C coating on the antibiocoorrosive and mechanical properties of different magnesium alloys. *Applied Surface Science* 2018, 427, pp. 617-627.
19. Patel K., Doyle C. S., Yonekura D., James B.J.: Effect of surface roughness parameters on thermally sprayed PEEK coatings. *Surface and Coatings Technology* 204(21-22), 2010, pp. 3567-3572.
20. Varacalle D.J., Guillen D.P., Deason D.M., Rhodaberger W., Sampson E.: Effect of Grit-Blasting on Substrate Roughness and Coating Adhesion. *Journal of Thermal Spray Technology* 2006, 15(3), pp. 348-355.

21. Abdulkareem M.H., Abdulateef N.E., Kadhim M.J.: Evaluation of Surface Roughness of 316L Stainless Steel Substrate on Nanohydroxyapatite by Electrophoretic Deposition. *Al-Nahrain Journal for Engineering Sciences* 2018, 21(1).
22. Jiang C., Jiang H., Zhang J., Kang G.: Analytical model of friction behavior during polymer scratching with conical tip. *Friction* 2018, 7(5), pp. 466–478.
23. Victrex VICOTE peek coating Technology Victrex 2017.
24. Plastics – Determination of hardness – Part 1: Ball indentation method, PN-EN ISO 2039-1, 2004.
25. Briscoe B.J., Fiori L., Pelillo E.: Nano-indentation of polymeric surfaces. *Journal of Physics D: Applied Physics* 1998, 31(19), pp. 2395–2405.
26. Mussert K.M., Vellinga W.P., Bakker A., Zwaag S.V.D.: A nano-indentation study on the mechanical behaviour of the matrix material in an AA6061 – Al₂O₃ MMC. *Journal of Materials Science* 2002, 37(4), pp. 789–794.
27. Roa J.J., Oncins G., Diaz J., Sanz F., Segarra M.: Calculation of Young's Modulus Value by Means of AFM. *Recent Patents on NanoTechnology* 2011, 5(1), pp. 27–36.
28. Guillonneau G., Kermouche G., Bec S., Loubet J.-L.: Determination of mechanical properties by nanoindentation independently of indentation depth measurement. *Journal of Materials Research* 2012, 27(19), pp. 2551–2560.
29. Kim G., Elnabawi O., Shin D., Pae E.K.: Transient Intermittent Hypoxia Exposure Disrupts Neonatal Bone Strength. *Front Pediatr* 2016, 4, p. 15.
30. Schiavi A., Origlia C., Germak A., Barbato G., Maizza G., Genta G., Cagliero R., Coppola G.: Indentation modulus at macro-scale level measured from Brinell and Vickers indenters by using the primary hardness standard machine at INRiM. *Acta Imeko* 2019, 8(1).
31. Standard Test Method for Evaluation of Scratch Resistance of Polymeric Coatings and Plastics Using an Instrumented Scratch Machine. ASTM D7027-13, 2013.
32. Zhang G., Li W., Cherigui M., Zhang C., Liao H., Bordes J.-M., Coddet C.: Structures and tribological performances of PEEK (poly-ether-ether-ketone)-based coatings designed for tribological application. *Progress in Organic Coatings* 2007, 60(1), pp. 39–44.
33. Moskalewicz T., Zimowski S., Zych A., Łukaszczyk A., Reczyńska K., Pamuła E.: Electrophoretic Deposition, Microstructure and Selected Properties of Composite Alumina/Polyetheretherketone Coatings on the Ti-13Nb-13Zr Alloy. *Journal of The Electrochemical Society* 2018, 165(3), D116-D128.
34. Frigione M., Naddeo C., Acierno D.: Crystallisation behavior and mechanical properties of poly(aryl ether ether ketone)/poly(ether imide) blends. *Polymer Engineering & Science* 1996, 36(16), pp. 2119–2128.
35. Zhang G., Liao H., Yu H., Ji V., Huang W., Mhaisalkar S. G., Coddet C.: Correlation of crystallisation behavior and mechanical properties of thermal sprayed PEEK coating. *Surface and Coatings Technology* 2006, 200(24), pp. 6690–6695.
36. Nieminen T., Kallela I., Wuolijoki E., Kainulainen H., Hiidenheimo I., Rantala I.: Amorphous and crystalline polyetheretherketone: Mechanical properties and tissue reactions during a 3-year follow-up. *J Biomed Mater Res A* 2008, 84(2), pp. 377–383.
37. Choupin T., Debertrand L., Fayolle B., Régnier G., Paris C., Cinquin J., Brulé B.: Influence of thermal history on the mechanical properties of poly(ether ketone ketone) copolymers. *Polymer Crystallisation* 2019, 2(6).
38. Alvaredo-Atienza A., Chen L., San-Miguel V., Ridruejo A., Fernandez-Blazquez J. P.: Fabrication and Characterization of PEEK/PEI Multilayer Composites. *Polymers (Basel)* 2020, 12(12).